Comparative Phosphoproteomics of Zebrafish Fyn/Yes Morpholino Knockdown Embryos*[S]

Simone Lemeer‡§, Chris Jopling‡¶, Joost Gouw§, Shabaz Mohammed§, Albert J. R. Heck§, Monique Slijper§, and Jeroen den Hertog‡‖

The coordinated movement of cells is indispensable for normal vertebrate gastrulation. Several important players and signaling pathways have been identified in convergence and extension (CE) cell movements during gastrulation, including non-canonical Wnt signaling. Fyn and Yes, members of the Src family of kinases, are key regulators of CE movements as well. Here we investigated signaling pathways in early development by comparison of the phosphoproteome of wild type zebrafish embryos with Fyn/Yes knockdown embryos that display specific CE cell movement defects. For quantitation we used differential stable isotope labeling by reductive amination of peptides. Equal amounts of labeled peptides from wild type and Fyn/Yes knockdown embryos were mixed and analyzed by on-line reversed phase TiO_2-reversed phase LC-MS/MS. Phosphorylated and non-phosphorylated peptides were quantified, and significant changes in protein expression and/or phosphorylation were detected. We identified 348 phosphoproteins of which 69 showed a decrease in phosphorylation in Fyn/Yes knockdown embryos and 72 showed an increase in phosphorylation. Among these phosphoproteins were known regulators of cell movements, including Adducin and PDLIM5. Our results indicate that quantitative phosphoproteomics combined with morpholino-mediated knockdowns can be used to identify novel signaling pathways that act in zebrafish development *in vivo*. *Molecular & Cellular Proteomics 7:2176–2187, 2008.*

In vertebrate gastrulation morphogenetic cell rearrangements coordinate the movement of the three germ layers, ultimately creating the basic body plan of the developing embryo. One of the major cell movements during gastrulation is convergence and extension (CE).[1] During CE movements, cells converge toward the midline of the embryo and extend along the anterior-posterior axis, a process that requires the precise regulation of cell polarity, cell migration, and cell division (1, 2). Forward and reverse genetics screens have provided insight into the many signaling pathways that drive CE cell movements during gastrulation (3). The non-canonical Wnt pathway has a central role in CE movements, and mutations in Wnt11 and Wnt5 result in CE cell movement defects (4, 5). Moreover gain or loss of function of positive and negative regulators of CE signaling result in severe gastrulation defects, indicating that precise control of cell movements is required (6, 7). Non-canonical Wnt signaling acts to activate several downstream effectors including the small GTPases, Rho, Rac, and Cdc42. In turn, Rho kinases mediate cytoskeletal dynamics by regulating actin-myosin contractility (8–10). In addition, several other regulators of Rho and Rac that are required for proper CE movements such as guanine nucleotide exchange factors (11, 12) and Has2 (13) have been identified. Morpholino-mediated double knockdown of Fyn and Yes also results in impaired CE cell movements. These knockdowns are specific as they are rescued by co-expression of Fyn and Yes. The Fyn/Yes knockdowns phenocopy mutations in Wnt11 and Wnt5 in zebrafish. These phenotypes are rescued by active RhoA, indicating that Wnt11 and Fyn/Yes converge on RhoA downstream in the signaling pathway (14). How all of these signaling pathways cooperate in CE cell movements remains to be determined.

Proteomics is a powerful method to study signaling pathways and associated post-translational modifications that propagate signals, such as protein phosphorylation. Recent advances in phosphoproteomics have made the global characterization of the phosphoproteome of a complete organism feasible (15–18). These studies have revealed an enormous amount of new phosphoproteins and phosphorylation sites and the relationships between those phosphoproteins. In addition, the global analysis of the phosphoproteome is used to study specific signaling pathways (19). However, to detect dynamic changes in the phosphoproteome, quantitative analysis is indispensable. Quantitation methods vary and are

From the ‡Hubrecht Institute-Royal Netherlands Academy of Arts and Sciences and University Medical Center Utrecht, Uppsalalaan 8, 3584 CT Utrecht, the Netherlands and §Biomolecular Mass Spectrometry and Proteomics Group, Bijvoet Center for Biomolecular Research and Utrecht Institute for Pharmaceutical Sciences, Utrecht University, Sorbonnelaan 16, 3584 CA Utrecht, the Netherlands

Received, February 22, 2008, and in revised form, May 22, 2008

Published, MCP Papers in Press, June 11, 2008, DOI 10.1074/mcp.M800081-MCP200

[1] The abbreviations used are: CE, convergence and extension; SILAC, stable isotope labeling by amino acids in cell culture; WT, wild type; RP, reversed phase; hpf, h postfertilization; SCX, strong cation exchange; IPI, International Protein Index; XIC, extracted ion chromatogram; PRIDE, proteomics identification; IGF2BP1, insulin-like growth factor 2 mRNA-binding protein 1; PI3K, phosphatidylinositol 3-kinase; FY, Fyn/Yes; GAP, GTPase-activating protein; SH3, Src homology 3; BIAP2L1, brain-specific angiogenesis inhibitor 1-associated protein 2-like1; COPA, coatomer protein complex subunit α.

based on two-dimensional gel electrophoresis (DIGE), chemical approaches (ICAT and isobaric tags for relative and absolute quantitation (iTRAQ)) or stable isotope labeling by amino acids in cell culture (SILAC) (20). Especially SILAC has proven to be successful to study changes in the phosphoproteome upon induction of signal transduction pathways. This labeling method has the advantage that after labeling cell states are mixed together and all other sample handlings are carried out simultaneously. However, the use of SILAC is limited to single cell cultures. Other methods use stable isotope metabolic labeling in which all amino acids and peptides are labeled by growing cells on media containing exclusively $^{14}N/^{15}N$ (21–23). This method is widely used for lower organisms such as yeast, but it was also shown to be effective in labeling higher organisms such as *Caenorhabditis elegans* and *Drosophila* by feeding them heavy and light labeled yeast (24). It is feasible to use metabolic labeling approaches for higher organisms such as rats (25). However, these approaches are not straightforward and are expensive. In contrast, relatively simple chemical labeling approaches have recently become available that, in principle, allow for the quantitation of any biological sample of interest.

Dimethyl labeling provides a relatively straightforward, cheap, and simple strategy to label samples. In stable isotope dimethyl labeling, primary amine groups (lysine and amino termini) of peptides are labeled with formaldehyde through reductive amination (26–28). Primary amines are isotopically labeled using either light formaldehyde or heavy (deuterium-containing) formaldehyde. Because trypsin is usually used as the enzyme for digestion, most peptides will contain at least one label because each amino terminus and each lysine becomes labeled.

Here we investigated signaling pathways and phosphorylation events involved in CE cell movements. Fyn/Yes knockdown impairs CE cell movements during gastrulation in zebrafish embryos. We questioned whether there are changes in the phosphoproteome of Fyn/Yes knockdown embryos compared with wild type (WT) embryos. We used a quantitative phosphoproteomics approach using stable isotope labeling by amination of tryptic peptides to detect changes in protein expression and protein phosphorylation upon morpholino-mediated knockdown of Fyn and Yes in zebrafish embryos. This approach led to the identification of phosphoproteins that were differentially regulated upon knockdown of Fyn and Yes, whereas the majority of phosphoproteins were not changed, indicating that the observed changes were specific. Interestingly among the differentially phosphorylated proteins were many proteins with known functions in gastrulation cell movements, such as Wnt signaling and Rho kinase signaling components.

MATERIALS AND METHODS

Zebrafish Embryos and Microinjections—Zebrafish were kept, and the embryos were staged as described before (29). Antisense morpholinos were ordered from GeneTools (Philomath, OR). The morpholinos were targeted close to the start ATG of the respective cDNAs, and their sequences have been described before (14). The Fyn and Yes morpholinos (4 ng each) were injected at the one-cell stage.

Sample Preparation—Embryos, 30 wild type (approximately 100 μg) and 30 Fyn/Yes knockdown (approximately 100 μg) (24 h post-fertilization (hpf)), were manually dechorionated and deyolked with deyolking buffer (½ Ginzburg Fish Ringer) without calcium (30). Subsequently embryos were lysed in 8 M urea, 25 mM ammonium bicarbonate containing 5 mM sodium phosphate, 1 mM potassium fluoride, 1 mM sodium orthovanadate, pH 8.2, and EDTA-free protease inhibitor mixture (Sigma). Homogenized lysates were centrifuged at 14,000 × *g* to pellet cellular debris. Lys-C (Roche Diagnostics) was added to the lysate, and digestion was performed for 4 h at 37 °C. Samples were reduced with DTT at a final concentration of 2 mM at 56 °C; subsequently samples were alkylated with iodoacetamide at a final concentration of 4 mM at 20 °C. The eluate was diluted to 2 M urea, 50 mM ammonium bicarbonate, and trypsin (Roche Diagnostics) was added. Digestion was performed overnight at 37 °C.

Stable Isotope Labeling by Amination of Tryptic Peptides—Tryptic peptides were desalted, dried *in vacuo*, and resuspended in 100 μl of triethylammonium bicarbonate (100 μM). Subsequently 4 μl of formaldehyde-H_2 (4% (v/v) in water) was added and vortexed for 2 min followed by the addition of 4 μl of freshly prepared sodium cyanoborohydride (600 mM). The resultant mixture was vortexed for 60 min at room temperature. 16 μl of ammonium hydroxide (1% in water) was added to consume the excess formaldehyde, and 5% formic acid (in water) was added to acidify the solution. For deuteromethylation labeling, formaldehyde-D_2 (4% (v/v) in water) was used. The light 4H- and heavy 4D-dimethyl-labeled samples were mixed in a 1:1 ratio based on total peptide amount determined by running an aliquot of the labeled samples on a regular LC-MS run and comparing overall peptide signal intensities.

Strong Cation Exchange—Strong cation exchange was performed using Zorbax BioSCX-Series II columns (0.8-mm inner diameter × 50-mm long; particle size, 3.5 μm), a Famos autosampler (LC Packings, Amsterdam, the Netherlands), a Shimadzu LC-9A binary pump, and an SPD-6A UV detector (Shimadzu, Tokyo, Japan). Prior to strong cation exchange (SCX) chromatography, the mixed and labeled digest was desalted using a small plug of C_{18} material (3M Empore C_{18} extraction disk) packed into a GELoader Tip as described previously (31). The eluate was dried completely by vacuum centrifugation and subsequently reconstituted in 20% acetonitrile and 0.05% formic acid. After injection, the first 10 min were run isocratically at 100% solvent A (0.05% formic acid in 8:2 (v/v) water/acetonitrile, pH 3.0) followed by a linear gradient of 1.3% min^{-1} solvent B (500 mM NaCl in 0.05% formic acid in 8:2 (v/v) water/acetonitrile, pH 3.0). A total number of 25 SCX fractions (1 min each, *i.e.* 50-μl elution volume) were manually collected and dried in a vacuum centrifuge.

Two-dimensional Nanoflow HPLC—Nanoflow LC-MS/MS was performed by coupling an Agilent 1100 HPLC system (Agilent Technologies, Waldbronn, Germany) to an Orbitrap mass spectrometer (Thermo Electron, Bremen, Germany). The trap column consists of three separate precolumns: a 30-mm long × 100-μm-inner diameter Aqua C_{18} precolumn followed by a 5-mm long × 100-μm-inner diameter TiO_2 precolumn followed by a 30-mm long × 100-μm-inner diameter Aqua precolumn. The "sandwich" precolumn is then coupled to a 200-mm long × 50-μm-inner diameter ReproSil-Pur C_{18}-AQ analytical column. Peptides are trapped at 5 μl/min in 100% solvent A (0.1 M acetic acid + 0.13 M formic acid in water) on the first 30-mm C_{18} trap column. The subsequent H_2O/ACN gradient elutes and separates bound peptides using the analytical column at a flow rate of ~100 nl/min. Phosphorylated peptides will pass through the TiO_2 precolumn at this flow rate and bind (32). All other peptides with no

TiO_2 affinity are chromatographically separated at ~100 nl/min in a 100-min gradient from 0 to 40% solvent B (80% acetonitrile, 0.1 M acetic acid, and 0.13 M formic acid). Elution of phosphorylated peptides is achieved by injection of 30 μl of 100 mM ammonium hydrogen bicarbonate, pH 9.0 (adjusted with ammonia) containing 10 mM sodium phosphate, 5 mM sodium orthovanadate, and 1 mM potassium fluoride followed by an injection of 20 μl of 5% formic acid. During a second H_2O/ACN gradient phosphopeptides are separated using the 200-mm analytical column at ~100 nl/min in a 100-min gradient from 0 to 40% solvent B (80% acetonitrile, 0.1 M acetic acid, and 0.13 M formic acid). The eluent was sprayed via distal coated emitter tips (New Objective) butt-connected to the analytical column. In between the high voltage supply, the Orbitrap, and the electrospray needle an additional 33-megaohm resistor was placed to reduce ion current.

Mass Spectrometry—The mass spectrometer was operated in data-dependent mode, automatically switching between MS, MS/MS, and neutral loss-driven MS^3 acquisition. Full-scan MS spectra (from *m/z* 300 to 1500) were acquired in the Orbitrap with a resolution of 60,000 at *m/z* 400 after accumulation to a target value of 500,000. The three most intense ions at a threshold above 5000 were selected for collision-induced fragmentation in the linear ion trap at a normalized collision energy of 35% after accumulation to a target value of 10,000. The data-dependent neutral loss settings were chosen to trigger an MS^3 event after a neutral loss of 49 ± 0.5 *m/z* units was detected in the most intense fragment ion.

Data Analysis—All MS^2 and MS^3 spectra were converted to single .dta files using Bioworks 3.3. An in-house developed Perl script was used to assign the original and accurate parent mass to all MS^3 spectra, enabling an accurate mass database search. All first and second LC-MS runs of all SCX fractions were searched using an in-house licensed MASCOT search engine (MASCOT (version 2.1.0) software platform (Matrix Science, London, UK)) against the zebrafish International Protein Index (IPI) database version 3.27 (41,506) with carbamidomethylcysteine and "light" methylation of peptide amino termini and lysine residues set as fixed modifications and protein *N*-acetylation, oxidized methionines, phosphorylation of serine or threonine, and "heavy" methylation of peptide amino termini and lysine residues set as variable modifications. Trypsin was specified as the proteolytic enzyme, and up to two missed cleavages were allowed. The mass tolerance of the precursor ion was set to 5 ppm, and that of fragment ions was set to 0.9 Da.

Quantitation was performed using an in-house dimethyl-adapted version of MSQuant (SourceForge, Inc.). Briefly peptide ratios were obtained by calculating the extracted ion chromatograms (XICs) of the light and heavy forms of the peptide using the monoisotopic peaks only. The total XIC for each of the peptide forms was obtained by summing the XIC in consecutive MS cycles for the duration of their respective LC-MS peaks in the total ion chromatogram using FT-MS scans. This total XIC was then used to compute the peptide ratio. Heavy and light labeled peptides were found to largely co-elute. Quantified proteins were normalized against the $\log_2$ of the median of all peptides quantified. An in-house developed program was used to determine standard deviation, and a Student's *t* test was performed to detect significant regulation ($p \leq 0.05$). Proteins for which the standard deviation and *p* value could be determined and with a MASCOT score ≥80 were accepted (listed in supplemental Table 1). At least one unique peptide per protein was identified, eliminating redundancy in the data set.

Individual MS/MS spectra from phosphopeptides were accepted for a MASCOT score ≥40 (*p* value ≤0.005). Justification of the threshold was as described before (18). All identified phosphopeptides that were differentially phosphorylated were manually validated.

To determine the false discovery rate in the data sets, we performed a MASCOT search against the decoy database. For a MASCOT peptide score of 40 ($p \leq 0.005$), the false discovery rate was estimated to be 0.41%. All raw data and annotated spectra were submitted to the PRIDE database.

RESULTS

Analysis of Differential Phosphorylation—To investigate signaling pathways that have a role in the regulation of CE cell movements, we set out to evaluate the changes in the phosphoproteome after morpholino-mediated knockdown of Fyn and Yes in 24-hpf zebrafish embryos. To quantitate the differences, we used stable isotope labeling by reductive amination of peptides derived from the two experimental conditions and on-line automated RP-TiO_2-RP-LC-MS/MS. The experimental procedures are described in detail under "Materials and Methods," and a schematic overview of the complete experimental approach is depicted in Fig. 1.

Zebrafish embryos were injected with Fyn/Yes morpholinos at the one-cell stage, inducing specific knockdown of protein expression. As shown previously, Fyn/Yes knockdown induced severe gastrulation defects, characterized by reduced extension of the embryonic axis and improper extension of the forebrain anterior to the eyes. The Fyn/Yes knockdown phenotype is specific because it is rescued by co-injection of synthetic RNA encoding Fyn and Yes (14). Moreover Fyn/Yes knockdown resulted in specific changes in protein tyrosine kinase activity profiles that were also rescued by co-injection of Fyn and Yes RNA (33). A representative picture of a WT and a Fyn/Yes knockdown embryo at 24 hpf is shown in Fig. 1*A*. At 24 hpf, 30 WT and 30 Fyn/Yes knockdown embryos were manually dechorionated, deyolked, pooled, and lysed. Protein mixtures were digested with trypsin and subsequently labeled with normal formaldehyde (CH_2O), light, for the WT embryos or deuteroformaldehyde (CD_2O), heavy, for the knockdown embryos. Samples were mixed in a 1:1 ratio (total peptide content). The resulting peptide mixture was first separated and fractionated by SCX chromatography, which, under acidic conditions, causes phosphopeptides to elute earlier than regular tryptic peptides (34). Resulting SCX fractions were subsequently subjected to our on-line RP-TiO_2-RP-LC-MS/MS enrichment setup (18, 32). The resulting peptides were analyzed by mass spectrometric detection using a linear ion trap (LTQ) orbitrap, and the MS/MS spectra were searched against the IPI zebrafish database using MASCOT to identify peptide sequence and phosphorylation sites. Finally peptide/protein ratios were determined using the intensities of heavy and light peptide pairs.

More than 1400 proteins were identified, quantified, and manually checked (supplemental Table 1). Quantified proteins were normalized against the $\log_2$ of the median of all peptides quantified. A Student's *t* test was performed to detect significant regulation. 555 proteins were shown to be significantly regulated ($p \leq 0.05$). Among the up-regulated proteins, Vitellogenins were found to be up-regulated in the Fyn/Yes knockdown. It is likely that this up-regulation of Vitellogenins is an

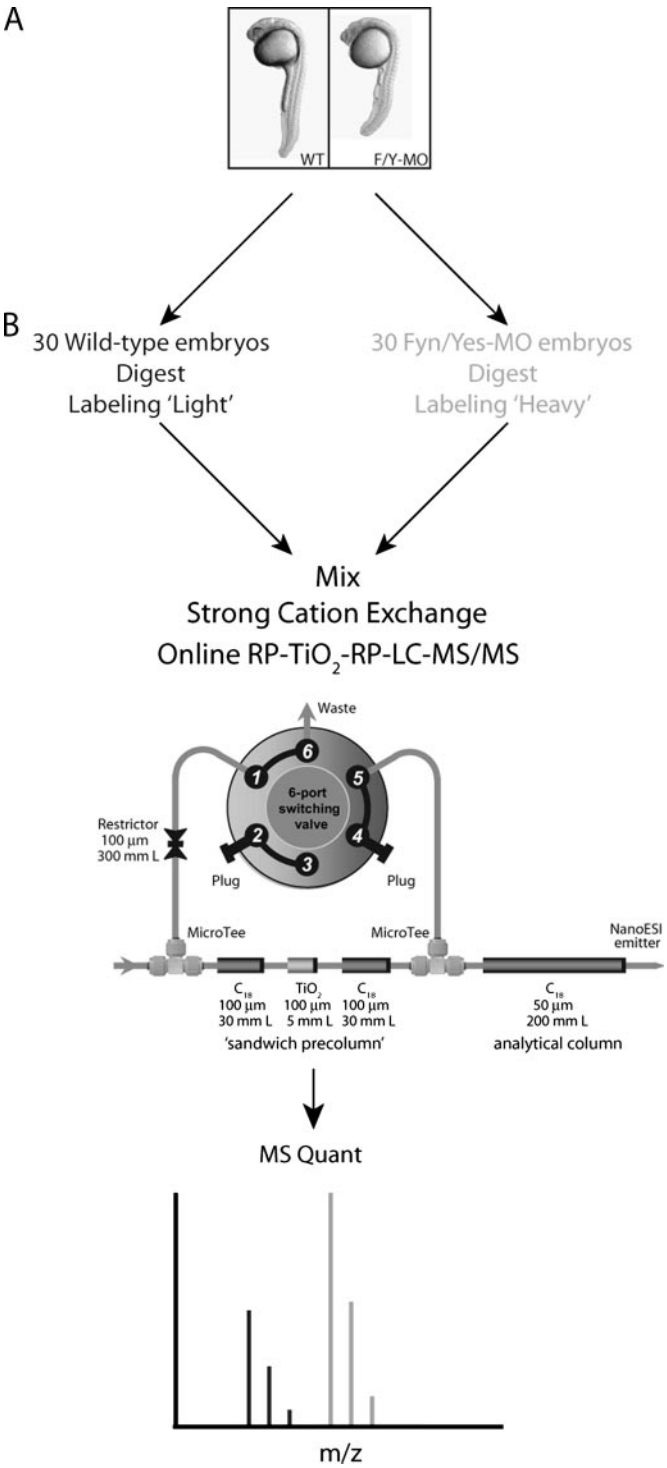

FIG. 1. **Experimental scheme for the analysis of changes in phosphorylation after morpholino-mediated knockdown of Fyn and Yes in zebrafish embryos.** *A*, lateral views of 1-day postfertilization wild type (*left*) and Fyn/Yes knockdown (*right*) zebrafish embryos. *B*, the lysates from WT and Fyn/Yes knockdowns were digested, and the resulting peptide mixtures were first labeled with light (WT) and heavy (FY) formaldehyde. Samples were mixed in a 1:1 ratio, and the mixture was separated by strong cation exchange chromatography. Each of the obtained SCX fractions was further analyzed by automated on-line RP-TiO_2-RP-LC-MS/MS. Peptides were analyzed and identified by MS^2 using a LTQ-Orbitrap mass spectrometer. Identified peptides were quantified by MSQuant and manually verified. *MO*, morpholino.

artifact of the manual deyolking procedure, and therefore we omitted Vitellogenins from further analyses. Skeletal muscle myosins and muscle actin were shown to be significantly down-regulated in the Fyn/Yes knockdown. Actomyosin contractility is known to be involved in gastrulation cell movements, which are controlled by Wnt signaling (35, 36). Although these results are potentially interesting, we focused on changes in protein phosphorylation upon knockdown of Fyn and Yes because these most likely reflect differences in signaling underlying CE cell movements.

All of the phosphopeptides that we detected were quantified by MSQuant and manually verified. Phosphopeptides and phosphoproteins were subsequently filtered based on their ratio and MASCOT score (≥40 and p value ≤0.005) and checked manually. After manual verification of the MS spectra and normalization, 348 phosphoproteins were validated. Table I shows a selection of differentially phosphorylated phosphopeptides that were identified with high confidence. We also determined the ratio of control, non-phosphorylated peptides that were derived from the proteins corresponding to the phosphopeptides. This allowed us to determine the relative protein expression level and the phosphorylation level and thus to discriminate between changes in protein levels and in phosphorylation state. The ratio of phosphorylation was determined multiple times, and the average is given in Table I as well as the number of peptides that were used to determine the ratio, the standard deviation, and p value. Similarly the average ratio of protein levels, number of peptides, and respective standard deviation and p value are provided. Some phosphopeptides were only identified and quantified once, whereas the corresponding protein ratio was based on multiple non-phosphorylated peptides (Table II, upper panel). Some proteins were identified and quantified based on phosphopeptides without information on the relative protein levels (Table II). In the latter cases we cannot exclude protein up- or down-regulation, but the absolute amount of phosphopeptide did change. A list of all phosphoproteins and the ratio of phosphorylation in Fyn/Yes knockdown and WT is available as supplemental Table 2. A list of all identified phosphopeptides (MASCOT score ≥40 and p value ≤0.005) including their MASCOT score is shown in supplemental Table 3. All annotated spectra were uploaded to the PRIDE database. Spectra of all phosphopeptides in Tables I and II are depicted in supplemental Figs. 1 and 2.

The differences in phosphorylation ratio of the phosphoproteins we identified are not as high as reported in other recent studies (37–39); this can be explained by the fact that we analyzed total embryo lysates. The Fyn/Yes knockdown will only affect certain cell types, and therefore the detected effect

TABLE I

Down- and up-regulated phosphopeptides after Fyn/Yes knockdown

Selected phosphopeptides and proteins showing differential phosphorylation are shown. Included in the table are phosphopeptide ratio, number of phosphopeptides used for quantitation, standard deviation (StDev), and *p* value. Also included are the protein ratio based on non-phosphorylated peptide, number of non-phosphorylated peptides used for quantitation, standard deviation, and *p* value.

IPI entry	Protein	Phosphopeptide	Phosphopeptide Ratio				Protein Ratio			
			Down							
IPI entry	Protein	Phosphopeptide	Ratio FY/WT	# of pept	StDev	Pvalue	Protein Ratio ‡	# of pept	StDev	Pvalue
IPI00507684	Beta-catenin 2	TpSMGGTQQQFVEGVR	0.73	4	0.13	0.028	0.96	3	0.03	0.133
IPI00800578	Insulin-like growth factor 2 mRNA-binding protein 1 (IGF2BP1)	QMpSPGSGIPSK	0.52	7	0.10	0.000	0.93	16	0.19	0.081
IPI00487372	Ras-GTPase activating protein SH3 domain-binding protein 2	ALpSPVPLESPPNIQEPPK	0.79	4	0.02	0.001	1.13	3	0.03	0.018
IPI00494222	Vimentin	ITpSPFPNFSSLSLR	0.68	2	0.06	0.107	0.56	3	0.04	0.005
IPI00481246	ctps CTP synthase	SGSSpSPDLEIADLK	0.70	4	0.03	0.001	1.13	4	0.07	0.033
IPI00500366	tcea1 Transcription elongation factor A (SII), 1	TTPVVSPSETpSPEPR	0.35	2	0.10	0.026	1.03	3	0.15	0.824
IPI00493027	Adducin 3	QEVVp(TT)PPPPSVGK	0.76	3	0.09	0.004	1.01	3	0.04	0.807
			Up							
IPI entry	Protein	Phosphopeptide	Ratio FY/WT	# of pept	StDev	Pvalue	Protein Ratio ‡	# of pept	StDev	Pvalue
IPI00509756	PDLIM5	SQPpSPNSISSPASNSAPKPSSGR	1.53	2	0.01	0.009	1.22	3	0.17	0.132
IPI00481806	Ribosomal protein S6 kinase alpha-3	NVpSPVLDPVGCSTLAQR	1.24	2	0.01	0.015	1.29	3	0.06	0.010
IPI00500409	Ras-GTPase activating protein SH3 domain-binding protein 2	GSTPGLALpTPPPQTPEPPK	1.30	3	0.03	0.001	1.23	4	0.01	0.000
IPI00488000	mitogen-activated protein kinase kinase 1	TMGLHQPp(ST)PTHSAE	1.32	6	0.02	0.000	1.11	9	0.16	0.069
IPI00834498	desmoplakin	GISSPYNVSpSGPSSR	1.86	2	0.16	0.066	1.48	4	0.19	0.003
IPI00488890	eIF4B	SIPKEEEQSGSVpSPQSNPTNTSR	1.71	7	0.47	0.002	1.04	15	0.19	0.650
IPI00495530	Titin-like	IVLSPpSMEAPK	1.84	8	0.17	0.000	0.86	9	0.20	0.049
			Unchanged							
IPI entry	Protein	Phosphopeptide	Ratio FY/WT	# of pept	StDev	Pvalue	Protein Ratio ‡	# of pept	StDev	Pvalue
IPI00509057	Coatomer protein complex subunit alpha	NLpSPGAVDTEVR	1.05	2	0.03	0.211	1.09	5	0.1	0.11

‡ Calculated with only non-phosphorylated peptides.

is less pronounced than in homogenous tissue culture cells that are treated with large amounts of growth factor. Nevertheless we detected changes in phosphorylation of proteins.

Decrease in Phosphorylation—Among the peptides with a decrease in phosphorylation upon Fyn/Yes knockdown, we identified the phosphopeptide QMpSPGSGIPSK (where pS is phosphoserine) from insulin-like growth factor 2 mRNA-binding protein 1 (IGF2BP1) with high confidence (MS^2 spectrum in Fig. 2*A*). The phosphopeptides were less abundant in the Fyn/Yes knockdown (0.52 ± 0.10). To monitor IGF2BP1 protein expression, we quantified the ratio of control non-phosphorylated peptides and found that the protein ratio was 0.93 ± 0.19 (Table I). Indeed equal amounts of non-phosphorylated peptide MILEIMNQEAK were detected in Fyn/Yes knockdown and WT lysates (Fig. 2*C*). Fig. 2 shows both the MS spectrum and the XIC of the phosphorylated (Fig. 2*B*) and non-phosphorylated (Fig. 2*C*) peptide. It was evident that the MS spectrum of the phosphorylated peptide in the Fyn/Yes knockdown (*gray*) was lower in intensity than in the WT (*black*). This was reflected in the XIC (Fig. 2*B*). In the control, non-phosphorylated peptide, the intensities are similar; this was also reflected in the XIC (Fig. 2*C*), indicating that phosphorylation but not abundance of IGF2BP1 protein levels was affected by Fyn/Yes knockdown.

IGF2BP1 is a member of the VICKZ family of RNA-binding proteins, and it regulates mRNA nuclear export, localization, stability, and translation. IGF2BP1 binds to the 5′-untranslated region of the insulin-like growth factor 2 mRNA thereby regulating its subcellular localization and translation. VICKZ proteins are highly conserved among all vertebrates and are expressed in embryonic cells. It is suggested that VICKZ proteins play a role in cell migration via the ability to localize RNA. Many human tumors overexpress VICKZ proteins (40). *Xenopus* xVICKZ3 is required for migration of cells that form the roof plate of the neural tube and for migration of neural crest cells (41). Taken together, IGF2BP1 likely has a role in cell migration during zebrafish development.

The phosphopeptide TpSMGGTQQQFVEGVR, corresponding to β-catenin, was also identified in our screen. The protein ratio of β-catenin did not change significantly upon Fyn/Yes knockdown (0.96 ± 0.03), whereas the identified phosphopeptides showed a decrease (0.73 ± 0.13) (Table I). The identified site is a reported Akt phosphorylation site (42). Akt is a direct downstream effector of phosphatidylinositol 3-kinase (PI3K). It is noteworthy that PI3K is involved in CE cell movements as treatment of zebrafish embryos with the PI3K inhibitor LY294002 induces defects in CE cell movements (43).

Another phosphopeptide that showed a significant decrease in phosphorylation was QEVVp(TT)PPPPSVGK (where pT is phosphothreonine) from Adducin 3 (0.76 ± 0.09). The protein ratio remained unchanged upon Fyn/Yes knockdown (1.01 ± 0.04) (Table I). The identified phosphorylation site of Adducin has not been reported previously, and the upstream kinase is unknown. Adducin is a membrane skeletal protein that binds to Actin. Previously it has been shown that phos-

TABLE II

Quantitation of single phosphopeptides and of phosphopeptides without protein ratios after Fyn/Yes knockdown

The upper panel shows selected phosphopeptides and proteins showing differential phosphorylation based on only one phosphopeptide. Included in the table are phosphopeptide ratio and total protein ratio based on non-phosphorylated peptides including number of non-phosphorylated peptides used for quantitation, standard deviation (StDev), and *p* value. The lower panel shows selected phosphopeptides showing differential phosphorylation, but non-phosphorylated peptides were not identified. Included in the table is phosphopeptide ratio including number of phosphorylated peptides used for quantitation, standard deviation, and *p* value.

Phosphopeptide ratio based on 1 phosphopeptide

IPI entry	Protein	Phosphopeptide	Phosphopeptide Ratio				Protein Ratio			
			Down							
IPI entry	Protein	Phosphopeptide	Ratio FY/WT	# of pept	StDev	Pvalue	Protein Ratio ‡	# of pept	StDev	Pvalue
IPI00551951	Transcription factor Sox-3	TEPp(SS)PPPAITSHSQR	0.62	1	x	x	0.54	2	0.03	0.046
IPI00494181	suppressor of ypt; emmental (Sly1) SCFD1	VSVDESHGSEApSPAGARPK	0.65	1	x	x	1.13	7	0.20	0.980
			Up							
IPI entry	Protein	Phosphopeptide	Ratio FY/WT	# of pept	StDev	Pvalue	Protein Ratio ‡	# of pept	StDev	Pvalue
IPI00616419	Gravin	EGILPWSpSFK	1.05	1	x	x	1.29	16	0.29	0.001
		VTASPDTSGEp(TT)PVPGDGVERK	1.75	1	x	x	1.29	16	0.29	0.001
IPI00492334	BCL-XL_like protein 1	TNASSTGpTPPQSPASSPQR	1.48	1	x	x	1.26	2	0.04	0.066

No protein ratio; only phosphopeptides identified

IPI entry	Protein	Phosphopeptide	Phosphopeptide Ratio				Protein Ratio
			Down				
IPI entry	Protein	Phosphopeptide	Ratio FY/WT	# of pept	StDev	Pvalue	Protein Ratio ‡
IPI00481249	similar to kaiso	SQIQPDSPNTASLpSPK	0.76	3	0.08	0.050	x
IPI00493419	Vacuolar protein sorting-associated protein 26B-A	SMpSQQATIAAQR	0.72	4	0.07	0.007	1.15 (1 pept)
IPI00512785	Metastasis associated 1 family, member 2 MTA2	QEVQGMpSPFTSSAGR	0.61	5	0.05	0.000	0.58 (1 pept)
IPI00799668	Synapsin	SQGPAVpSPQPISQSR	0.59	2	0.02	0.022	x
			Up				
IPI entry	Protein	Phosphopeptide	Ratio FY/WT	# of pept	StDev	Pvalue	Protein Ratio ‡
IPI00506241	BAIAP2	TSMSVIPESpSPTLER	1.35	7	0.10	0.000	x
IPI00570158	BAIAP2	TPVSNTPQPpSPSLQR	1.36	3	0.11	0.021	x
IPI00618202	TIF-1A	SVGpSPPISFLQRPF	2.49	2	0.04	0.00026	x
IPI00489143	DOCK7	SLSNpSNPDISGTPTSPDDEVR	1.34	1		0.036*	x
		SPpSGSAFGSQENLR	1.34	2	0.18	0.036*	x

* *p* value based on all phosphopeptides.

X Standard deviation, *p* value, and protein ratio cannot be determined; ratio is based on one (phospho)peptide.

‡ Calculated with only non-phosphorylated peptides.

phorylation of Adducin by protein kinase C and Rho kinase is implicated in cell motility, spreading, and migration (44). Therefore, it is likely that Adducin has a role in CE cell movements. Whether phosphorylation of the newly identified site also has a role in this process remains to be determined.

Vimentin protein expression and phosphorylation were both shown to be down-regulated upon Fyn/Yes knockdown (0.56 ± 0.04 and 0.68 ± 0.06, respectively) (Table I). Vimentin shows a high degree of sequence homology between species and is highly phosphorylated. Phosphorylation of Vimentin has been related to its function in cell adhesion, migration, and signaling (45), and reduced Vimentin protein levels and phosphorylation may therefore have a role in CE cell movements.

Among the peptides that were less phosphorylated upon Fyn/Yes knockdown, we identified a single phosphopeptide of Sly1 (Suppressor of Ypt) (FY/WT ratio, 0.65; Table II) encompassing a phosphorylation site that had not been reported before. Sly1 protein levels were not affected by Fyn/Yes knockdown (protein ratio, 1.13 ± 0.20; Table II). Sly1 is the vertebrate homologue of Sly1p in yeast. It is known to bind and regulate syntaxin 5 in vesicle transport from the endoplasmic reticulum to the Golgi (46). It also interacts with the small GTPase Rab (Ypt1p in yeast), a key regulator of protein transport in eukaryotic cells. Sly1 is involved in vesicle motility and docking as well as in membrane remodeling and fusion. In zebrafish, Sly1 was shown to be necessary for cell proliferation in fin regeneration (47). It will be interesting to investigate the role of phosphorylation in Sly1 function.

Phosphorylation of the Kaiso phosphopeptide SQIQPDSPNTASLpSPK was shown to decrease upon Fyn/Yes knockdown (FY/WT ratio, 0.76 ± 0.08), but we did not detect non-phosphorylated control peptides for Kaiso (Table II). Kaiso is a dual specificity transcriptional repressor that was identified to associate with p120-catenin. Kaiso is required for *Xenopus* gastrulation movements, and depletion of Kaiso results in the increased expression of non-canonical Wnt11, a regulator of CE cell movements (48). The identified phos-

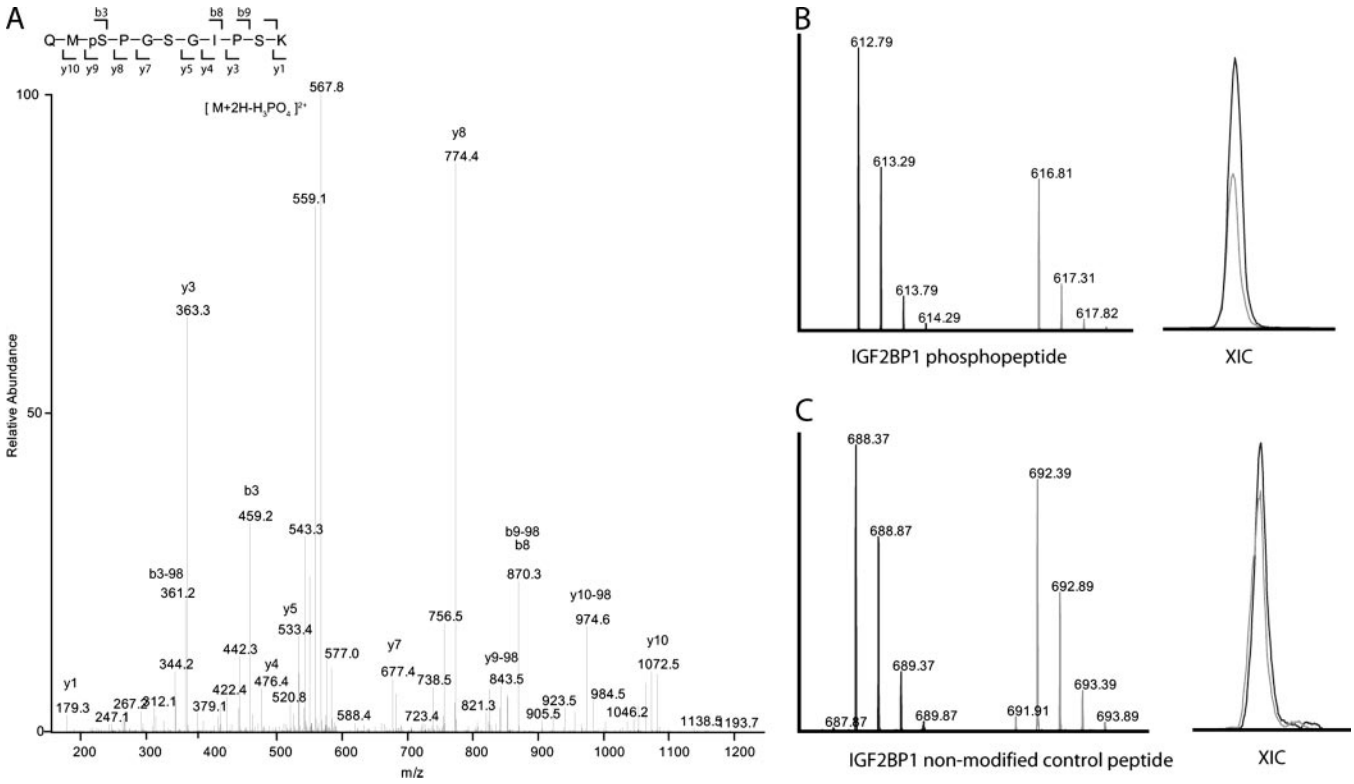

FIG. 2. **Phosphorylation of QMpSPGSGIPSK from insulin-like growth factor 2 mRNA-binding protein 1 is down-regulated in the Fyn/Yes knockdown.** *A*, MS^2 spectrum of QMpSPGSGIPSK from IGF2BP1. *B*, MS spectrum and XIC showing decrease of the phosphopeptide. *C*, the non-phosphorylated peptide MILEIMNQEAK from IGF2BP1 shows a close to 1:1 ratio in both the MS spectrum and XIC.

phopeptide is predicted to become phosphorylated by CDK5 (Scansite), and it will be interesting to see whether phosphorylation of this site results in functional changes in Kaiso-mediated signaling in gastrulation cell movements.

Increase in Phosphorylation—The phosphopeptide SQPpSPNSISSPASNSAPKPSSGR from PDLIM5 was shown to be increased upon Fyn/Yes knockdown (1.53 ± 0.01; Table I; see also MS^2 spectrum in Fig. 3*A*). The protein ratio, based on control non-phosphorylated peptides, also showed a slight up-regulation compared with WT although less strong than the phosphopeptides (1.22 ± 0.17; Table I). The MS spectrum of the phosphorylated peptide in the Fyn/Yes knockdown (*gray*) was much higher in intensity than in the WT (*black*). This was also reflected in the XIC (Fig. 3*B*). In one of the non-phosphorylated peptides, LIEDTEDWHPR, the intensities were similar, and this was reflected in the XIC (Fig. 3*C*). PDZ/LIM proteins have important roles in various cellular processes. PDLIM5 belongs to the Enigma subfamily of PDZ/LIM proteins that contain one PDZ and three LIM domains (49). In zebrafish, Enigma knockdown results in embryonic lethality shortly after the end of gastrulation, and embryos show elongation defects and disorganized somites, suggesting a role for Enigma in cytoskeleton and somite organization during embryonic development (50).

Two phosphopeptides of Gravin/AKAP12 were identified. The ratio of one of the phosphopeptides increased (1.75), whereas the other phosphopeptide remained unchanged (1.05). The protein level increased somewhat (1.29 ± 0.29) upon Fyn/Yes knockdown (Table II). Gravin was recently shown to be involved in axis elongation during zebrafish gastrulation. It is thought to function as a scaffolding protein that promotes cell changes. Upon morpholino-mediated knockdown of Gravin, cells migrate normally to the dorsal side of the embryo but fail to extend properly along the anterior-posterior axis (51). It is conceivable that Gravin mediates some of the effects of Fyn and Yes in gastrulation cell movements.

Two different phosphopeptides that we identified matched the Ras-GTPase-activating protein (GAP) SH3 domain-binding protein 2 (IPI00500409 and IPI004873772). Phosphorylation of one of these proteins was decreased (0.79 ± 0.02), whereas phosphorylation of the other was increased (1.30 ± 0.03) (Table I). Control peptides of both of these proteins were slightly increased in response to Fyn/Yes knockdown (1.13 ± 0.03 and 1.11 ± 0.16, respectively; Table I). Alignment of the sequences of these two Ras-GAP SH3-binding protein 2 proteins indicated that they share 63% identity, and the phosphopeptides are clearly distinct. Ras-GAPs enhance the hydrolysis of bound GTP to GDP, leading to inactivation of Ras, and it is likely that these two Ras-GAP SH3 domain-binding proteins regulate Ras-GAP activity. Yet the role of (de)phosphorylation of these proteins in the process remains to be determined, and the finding that phosphorylation of one of

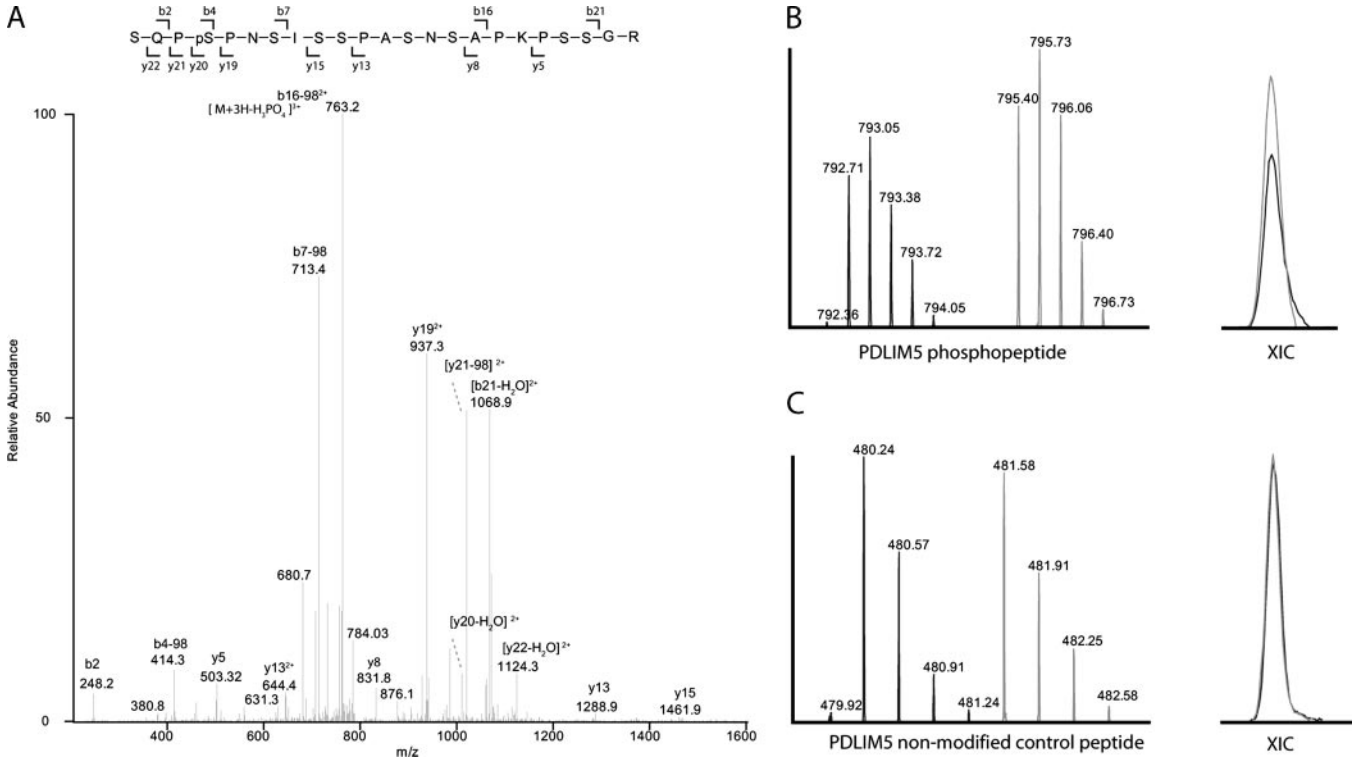

FIG. 3. **Phosphorylation of SQPpSPNSISSPASNSAPKPSSGR from PDLIM5 is up-regulated in the Fyn/Yes knockdown.** *A*, MS^2 spectrum of SQPpSPNSISSPASNSAPKPSSGR from PDLIM5. *B*, MS spectrum and XIC showing an increase of the phosphopeptide. *C*, a non-phosphorylated peptide, LIEDTEDWHPR, from PDLIM5 shows a close to 1:1 ratio in both the MS spectrum and XIC.

these proteins is up-regulated and phosphorylation of the other is down-regulated in response to Fyn/Yes knockdown is intriguing.

Two phosphopeptides of two isoforms of brain-specific angiogenesis inhibitor 1-associated protein 2-like1 (BIAP2L1A/BIAP2L1B) were identified, and phosphorylation of both peptides was enhanced upon Fyn/Yes knockdown (1.35 ± 0.10 and 1.36 ± 0.11, respectively) (Table II). Only the phosphopeptides could be identified, so up-regulation of the protein itself cannot be excluded. The phosphosite in BIAP2L1A is a potential substrate of GSK-3 as predicted by Scansite. The BIAP2L1A/B protein contains an evolutionarily conserved insulin receptor tyrosine kinase substrate p53 homology domain (IRSp53/MIM) that is known to bundle actin filaments and interact with the small GTPase Rac (52).

Two unique phosphopeptides of DOCK7 were enhanced upon Fyn/Yes knockdown (1.34 and 1.34 ± 0.18), but up-regulation of the protein itself cannot be excluded because control peptides were not identified in the sample (Table II). DOCK7 is a Rac activator and is a key regulator of axon formation. DOCK7 and Rac activation lead to the phosphorylation and subsequent inactivation of stathmin/Op18, a microtubule-destabilizing protein (53, 54). DOCK7 has been proposed to be a guanine nucleotide exchange factor not only for Rac but also for Rheb, transforming the GDP-bound Rheb into the GTP-bound state, although there is no direct evidence (55). From our data it is evident that phosphorylation of this regulator of small GTPases is affected by Fyn/Yes knockdown.

No Change in Phosphorylation upon Fyn/Yes Knockdown—It is noteworthy that the majority of phosphopeptides and protein levels did not change upon Fyn/Yes knockdown. The ratios of phosphorylation of 207 of the 348 phosphoproteins (62%) were shown to be distributed between 0.8 and 1.2 (Fig. 4). The phosphopeptide NLpSPGAVDTEVR (MS^2 spectrum shown in Fig. 5*A*) from the coatomer protein complex subunit α (COPA) did not show significant changes upon Fyn/Yes knockdown (1.04 ± 0.06) (Table I and Fig. 5*B*). The peptide ratio of control peptides from COPA was also unchanged (1.21 ± 0.05) (Table I). For instance, the non-phosphorylated control peptide CPLSGACYCPK is shown in Fig. 5*C*. Both phosphorylated and non-phosphorylated peptides from COPA, which is involved in cell cycle control, were not affected upon knockdown of Fyn and Yes.

DISCUSSION

Here we probed *in vivo* changes in protein phosphorylation upon knockdown of Fyn and Yes using RP-TiO_2-RP-LC-MS/MS. For quantification, we used stable isotope labeling by reductive amination of peptides as an alternative to stable isotope labeling of an entire zebrafish (embryo). Our procedure was efficient and robust, and the ratio of most phos-

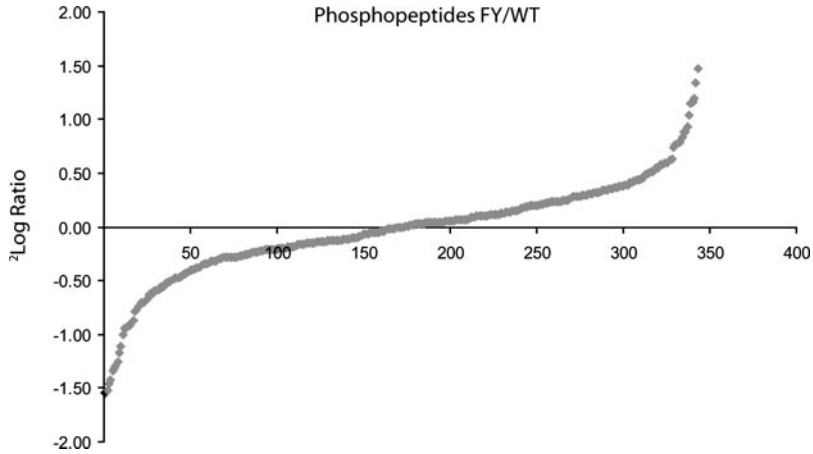

FIG. 4. **Normalized ratios of phosphopeptides.** The $\log_2$ of the normalized ratios of phosphopeptides is shown to be distributed around 0 in Fyn/Yes knockdown.

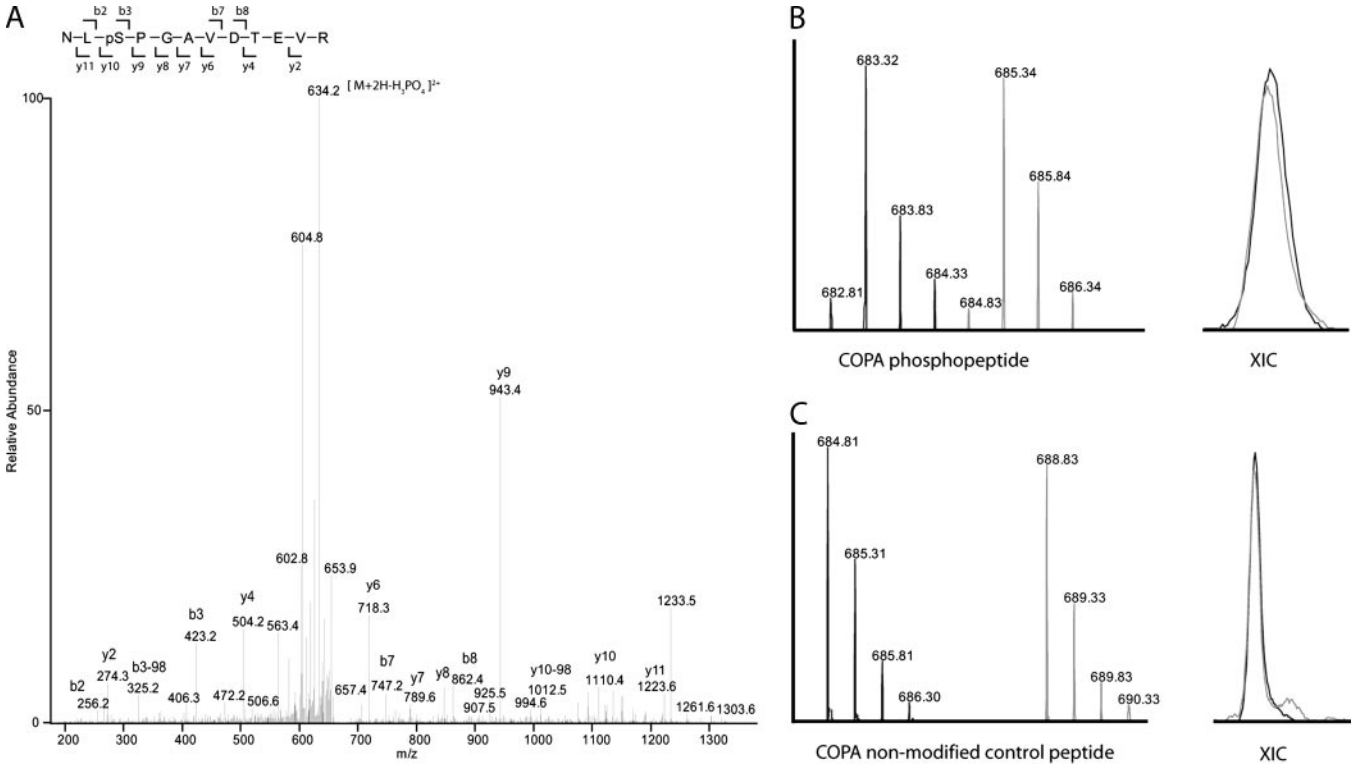

FIG. 5. **No change in phosphorylation in the phosphopeptide NLpSPGAVDTEV from COPA.** *A*, MS^2 spectrum of NLpSPGAVDTEVR of COPA. Both the phosphopeptide (*B*) and a control, non-phosphorylated peptide from COPA, CPLSGACYCPK (*C*), show a close to 1:1 ratio in both the MS spectrum and XIC.

phopeptides was between 0.8 and 1.2, *i.e.* phosphorylation of most proteins did not change significantly upon Fyn/Yes knockdown (Fig. 4). Yet a subset of phosphopeptides was differentially phosphorylated between wild type and Fyn/Yes knockdown embryos. For the identified phosphopeptides different, non-phosphorylated peptides of the same protein were quantified. This internal control for protein expression boosted confidence in the observed differences in phosphorylation. For some phosphopeptides, corresponding non-phosphorylated peptides were not detected (Table II). This is probably because of high enrichment of phosphopeptides by the TiO_2 column. Non-phosphorylated peptides of these proteins were not detected in the unbound fraction because of undersampling in the mass spectrometer. Low abundance phosphoproteins were therefore only quantified based on their phosphopeptides.

Taken together, stable isotope reductive amination is a fast and reliable alternative for metabolic stable isotope labeling of whole animals, and it can be used to quantify differences in protein phosphorylation between experimental samples. Moreover the reductive amination method is amenable to quantify and compare differences between any two sets of

proteins or protein mixtures, and it can be used as an inexpensive alternative to SILAC and stable isotope labeling of whole animals (27, 28).

Significant changes in both protein expression and protein phosphorylation were detected. We focused on the changes in phosphorylation upon Fyn/Yes knockdown because these are likely to represent the signaling pathways that have a role in CE cell movements. The changes in phosphorylation ratios were not as high as reported in previous studies (37–39); this presumably is the consequence of the mixed cell population that we used in this study as opposed to the homogenous cell cultures used in previous studies. The Fyn/Yes knockdown will not affect every cell type in the developing zebrafish embryo, and hence the differences in protein phosphorylation will be masked partially by the contribution of cells that are not affected by Fyn/Yes knockdown.

Nevertheless we detected significant changes in phosphopeptides. The phosphorylation of 141 of the 348 phosphoproteins was altered by Fyn/Yes knockdown (72 up and 69 down) (supplemental Table 2). Interestingly a subset of the phosphoproteins that were regulated by Fyn/Yes knockdown were known regulators of gastrulation cell movements (Kaiso, PDLIM5, and Gravin), actin cytoskeleton reorganization (Adducin and BIAP2L1A/B), and Wnt signaling pathways (β-catenin, Sox-3, and Kaiso) or were implicated in small GTPase signaling (Sly1, Ras-GAP SH3BP2, and DOCK7) (Tables I and II). The high amount of small GTPase regulators that showed a change in phosphorylation suggests a change in the balance of Rho and Rac activity upon Fyn/Yes knockdown. This is consistent with previous work demonstrating that CE cell movements are tightly regulated by small GTPases (3). CE cell movement defects in gastrulation upon Fyn/Yes knockdown are rescued by active RhoA (14), demonstrating that Rho signaling indeed is downstream of Fyn and Yes in gastrulation cell movements. Whether and, if so, how changes in the phosphorylation state of these proteins affects their activities remain to be determined. Nevertheless it is striking that differences in phosphorylation were detected in these known regulators of CE cell movements upon Fyn/Yes knockdown. The phosphorylation of many other proteins was altered upon Fyn/Yes knockdown as well. We analyzed our entire data set for predictions of involvement of kinases and kinase networks by bioinformatics approaches using the Search Tool for the Retrieval of Interacting Genes/Proteins (STRING) (European Molecular Biology Laboratory). These attempts did not result in a wealth of data most likely because of poor annotation of the zebrafish IPI database. This will certainly improve in the coming years, and with our data publicly deposited it will be interesting to see what the function is of the phosphoproteins that we identified in CE cell movements and/or Fyn/Yes signaling.

Fyn and Yes are members of the Src family of tyrosine kinases. However, we did not detect changes in tyrosine phosphorylation of downstream targets. This is primarily because of the low abundance of tyrosine phosphorylation in general and the mixed cell population used in this endogenous sample. We have shown previously using an immunoaffinity approach with anti-Tyr(P) antibodies that tyrosine phosphorylation is detectable in early zebrafish embryos (56). However, the amount of material that was required for those experiments (~2000 embryos per sample) would either require a significant scale-up of the morpholino injections or further refinement of the technology to allow detection of phosphotyrosine-containing proteins in Fyn/Yes knockdown embryos. The aim of the work described here was not to detect direct substrates of Fyn and Yes but rather to identify components of signaling pathways that have a role in CE cell movements.

Future research will be aimed at elucidating the role of Fyn and Yes signaling in gastrulation cell movements. It will be interesting to compare signaling between the Fyn/Yes knockdown embryos and non-canonical Wnt knockdown embryos. We have found recently that there is a significant overlap in the kinase activity profiles of Fyn/Yes and Wnt11 knockdowns (33), suggesting that indeed Fyn/Yes and Wnt11 signaling overlap. The large number of signaling proteins and novel proteins with altered phosphorylation upon Fyn/Yes knockdown warrants further investigation of the role of these proteins and of their phosphorylation in CE cell movements. Quantitative phosphoproteomics on zebrafish knockdown embryos as described here provides many new leads for the analysis of the role of these proteins in gastrulation cell movements.

* This work was supported by a grant from the Netherlands organization for scientific research (NWO Grant 015.001.131), European Union Research Training Network HPRN-CT-2000-00085, and the Netherlands Proteomics Centre. The costs of publication of this article were defrayed in part by the payment of page charges. This article must therefore be hereby marked "*advertisement*" in accordance with 18 U.S.C. Section 1734 solely to indicate this fact.

S The on-line version of this article (available at http://www.mcponline.org) contains supplemental material.

Raw mass spectrometry data have been deposited in the proteomics identification, PRIDE, database (www.ebi.ac.uk/pride) under accession numbers 3281–3291, 3297, 3299, and 3300–3316.

¶ Present address: Centre de Medicina Regenerativa de Barcelona, Dr. Aiguader 88, E-08003 Barcelona, Spain.

‖ To whom correspondence should be addressed. Tel.: 31-30-2121800; Fax: 31-30-2516464; E-mail: j.denhertog@niob.knaw.nl.

REFERENCES

1. Keller, R. (2002) Shaping the vertebrate body plan by polarized embryonic cell movements. *Science* **298,** 1950–1954
2. Solnica-Krezel, L. (2005) Conserved patterns of cell movements during vertebrate gastrulation. *Curr. Biol.* **15,** R213–R228
3. Solnica-Krezel, L. (2006) Gastrulation in zebrafish—all just about adhesion? *Curr. Opin. Genet. Dev.* **16,** 433–441
4. Heisenberg, C. P., Tada, M., Rauch, G. J., Saude, L., Concha, M. L., Geisler, R., Stemple, D. L., Smith, J. C., and Wilson, S. W. (2000) Silberblick/Wnt11 mediates convergent extension movements during zebrafish gastrulation. *Nature* **405,** 76–81
5. Kilian, B., Mansukoski, H., Barbosa, F. C., Ulrich, F., Tada, M., and Heisenberg, C. P. (2003) The role of Ppt/Wnt5 in regulating cell shape and movement during zebrafish gastrulation. *Mech. Dev.* **120,** 467–476

6. Topczewski, J., Sepich, D. S., Myers, D. C., Walker, C., Amores, A., Lele, Z., Hammerschmidt, M., Postlethwait, J., and Solnica-Krezel, L. (2001) The zebrafish glypican knypek controls cell polarity during gastrulation movements of convergent extension. *Dev. Cell* **1,** 251–264
7. Carreira-Barbosa, F., Concha, M. L., Takeuchi, M., Ueno, N., Wilson, S. W., and Tada, M. (2003) Prickle 1 regulates cell movements during gastrulation and neuronal migration in zebrafish. *Development* **130,** 4037–4046
8. Habas, R., Dawid, I. B., and He, X. (2003) Coactivation of Rac and Rho by Wnt/Frizzled signaling is required for vertebrate gastrulation. *Genes Dev.* **17,** 295–309
9. Habas, R., Kato, Y., and He, X. (2001) Wnt/Frizzled activation of Rho regulates vertebrate gastrulation and requires a novel Formin homology protein Daam1. *Cell* **107,** 843–854
10. Choi, S. C., and Han, J. K. (2002) Xenopus Cdc42 regulates convergent extension movements during gastrulation through Wnt/Ca^{2+} signaling pathway. *Dev. Biol.* **244,** 342–357
11. Daggett, D. F., Boyd, C. A., Gautier, P., Bryson-Richardson, R. J., Thisse, C., Thisse, B., Amacher, S. L., and Currie, P. D. (2004) Developmentally restricted actin-regulatory molecules control morphogenetic cell movements in the zebrafish gastrula. *Curr. Biol.* **14,** 1632–1638
12. Miyakoshi, A., Ueno, N., and Kinoshita, N. (2004) Rho guanine nucleotide exchange factor xNET1 implicated in gastrulation movements during Xenopus development. *Differentiation* **72,** 48–55
13. Bakkers, J., Kramer, C., Pothof, J., Quaedvlieg, N. E., Spaink, H. P., and Hammerschmidt, M. (2004) Has2 is required upstream of Rac1 to govern dorsal migration of lateral cells during zebrafish gastrulation. *Development* **131,** 525–537
14. Jopling, C., and den Hertog, J. (2005) Fyn/Yes and non-canonical Wnt signalling converge on RhoA in vertebrate gastrulation cell movements. *EMBO Rep.* **6,** 426–431
15. Mann, M., and Jensen, O. N. (2003) Proteomic analysis of post-translational modifications. *Nat. Biotechnol.* **21,** 255–261
16. Mumby, M., and Brekken, D. (2005) Phosphoproteomics: new insights into cellular signaling. *Genome Biol.* **6,** 230
17. Ptacek, J., and Snyder, M. (2006) Charging it up: global analysis of protein phosphorylation. *Trends Genet.* **22,** 545–554
18. Lemeer, S., Pinkse, M. W., Mohammed, S., van Breukelen, B., den Hertog, J., Slijper, M., and Heck, A. J. (2008) Online automated in vivo zebrafish phosphoproteomics: from large-scale analysis down to a single embryo. *J. Proteome Res.* **7,** 1555–1564
19. Olsen, J. V., Blagoev, B., Gnad, F., Macek, B., Kumar, C., Mortensen, P., and Mann, M. (2006) Global, in vivo, and site-specific phosphorylation dynamics in signaling networks. *Cell* **127,** 635–648
20. Ong, S. E., and Mann, M. (2007) Stable isotope labeling by amino acids in cell culture for quantitative proteomics. *Methods Mol. Biol.* **359,** 37–52
21. Oda, Y., Huang, K., Cross, F. R., Cowburn, D., and Chait, B. T. (1999) Accurate quantitation of protein expression and site-specific phosphorylation. *Proc. Natl. Acad. Sci. U. S. A.* **96,** 6591–6596
22. Conrads, T. P., Alving, K., Veenstra, T. D., Belov, M. E., Anderson, G. A., Anderson, D. J., Lipton, M. S., Pasa-Tolic, L., Udseth, H. R., Chrisler, W. B., Thrall, B. D., and Smith, R. D. (2001) Quantitative analysis of bacterial and mammalian proteomes using a combination of cysteine affinity tags and ^{15}N-metabolic labeling. *Anal. Chem.* **73,** 2132–2139
23. Benschop, J. J., Mohammed, S., O'Flaherty, M., Heck, A. J., Slijper, M., and Menke, F. L. (2007) Quantitative phosphoproteomics of early elicitor signaling in Arabidopsis. *Mol. Cell. Proteomics* **6,** 1198–1214
24. Krijgsveld, J., Ketting, R. F., Mahmoudi, T., Johansen, J., Artal-Sanz, M., Verrijzer, C. P., Plasterk, R. H., and Heck, A. J. (2003) Metabolic labeling of C. elegans and D. melanogaster for quantitative proteomics. *Nat. Biotechnol.* **21,** 927–931
25. Wu, C. C., MacCoss, M. J., Howell, K. E., Matthews, D. E., and Yates, J. R., III (2004) Metabolic labeling of mammalian organisms with stable isotopes for quantitative proteomic analysis. *Anal. Chem.* **76,** 4951–4959
26. Hsu, J. L., Huang, S. Y., Chow, N. H., and Chen, S. H. (2003) Stable-isotope dimethyl labeling for quantitative proteomics. *Anal. Chem.* **75,** 6843–6852
27. Huang, S. Y., Tsai, M. L., Chen, G. Y., Wu, C. J., and Chen, S. H. (2007) A systematic MS-based approach for identifying in vitro substrates of PKA and PKG in rat uteri. *J. Proteome Res.* **6,** 2674–2684
28. Huang, S. Y., Tsai, M. L., Wu, C. J., Hsu, J. L., Ho, S. H., and Chen, S. H. (2006) Quantitation of protein phosphorylation in pregnant rat uteri using stable isotope dimethyl labeling coupled with IMAC. *Proteomics* **6,** 1722–1734
29. Westerfield, M. (1995) *The Zebrafish Book. A Guide for the Laboratory Use of the Zebrafish (Danio rerio)*, 4th Ed., Univ. of Oregon Press, Eugene, OR
30. Link, V., Shevchenko, A., and Heisenberg, C. P. (2006) Proteomics of early zebrafish embryos. *BMC Dev. Biol.* **6,** 1
31. Gobom, J., Nordhoff, E., Mirgorodskaya, E., Ekman, R., and Roepstorff, P. (1999) Sample purification and preparation technique based on nano-scale reversed-phase columns for the sensitive analysis of complex peptide mixtures by matrix-assisted laser desorption/ionization mass spectrometry. *J. Mass Spectrom.* **34,** 105–116
32. Pinkse, M. W., Mohammed, S., Gouw, J. W., van Breukelen, B., Vos, H. R., and Heck, A. J. (2008) Highly robust, automated, and sensitive online TiO_2-based phosphoproteomics applied to study endogenous phosphorylation in Drosophila melanogaster. *J. Proteome Res.* **7,** 687–697
33. Lemeer, S., Jopling, C., Naji, F., Ruijtenbeek, R., Slijper, M., Heck, A. J., and den Hertog, J. (2007) Protein-tyrosine kinase activity profiling in knock down zebrafish embryos. *PLoS ONE* **2,** e581
34. Beausoleil, S. A., Jedrychowski, M., Schwartz, D., Elias, J. E., Villen, J., Li, J., Cohn, M. A., Cantley, L. C., and Gygi, S. P. (2004) Large-scale characterization of HeLa cell nuclear phosphoproteins. *Proc. Natl. Acad. Sci. U. S. A.* **101,** 12130–12135
35. Lee, J. Y., and Harland, R. M. (2007) Actomyosin contractility and microtubules drive apical constriction in Xenopus bottle cells. *Dev. Biol.* **311,** 40–52
36. Lee, J. Y., Marston, D. J., Walston, T., Hardin, J., Halberstadt, A., and Goldstein, B. (2006) Wnt/Frizzled signaling controls C. elegans gastrulation by activating actomyosin contractility. *Curr. Biol.* **16,** 1986–1997
37. Zhang, G., Spellman, D. S., Skolnik, E. Y., and Neubert, T. A. (2006) Quantitative phosphotyrosine proteomics of EphB2 signaling by stable isotope labeling with amino acids in cell culture (SILAC). *J. Proteome Res.* **5,** 581–588
38. Kratchmarova, I., Blagoev, B., Haack-Sorensen, M., Kassem, M., and Mann, M. (2005) Mechanism of divergent growth factor effects in mesenchymal stem cell differentiation. *Science* **308,** 1472–1477
39. Gruhler, A., Olsen, J. V., Mohammed, S., Mortensen, P., Faergeman, N. J., Mann, M., and Jensen, O. N. (2005) Quantitative phosphoproteomics applied to the yeast pheromone signaling pathway. *Mol. Cell. Proteomics* **4,** 310–327
40. Yaniv, K., and Yisraeli, J. K. (2002) The involvement of a conserved family of RNA binding proteins in embryonic development and carcinogenesis. *Gene* (*Amst.*) **287,** 49–54
41. Yaniv, K., Fainsod, A., Kalcheim, C., and Yisraeli, J. K. (2003) The RNA-binding protein Vg1 RBP is required for cell migration during early neural development. *Development* **130,** 5649–5661
42. He, X. C., Yin, T., Grindley, J. C., Tian, Q., Sato, T., Tao, W. A., Dirisina, R., Porter-Westpfahl, K. S., Hembree, M., Johnson, T., Wiedemann, L. M., Barrett, T. A., Hood, L., Wu, H., and Li, L. (2007) PTEN-deficient intestinal stem cells initiate intestinal polyposis. *Nat. Genet.* **39,** 189–198
43. Cha, Y. I., Kim, S. H., Sepich, D., Buchanan, F. G., Solnica-Krezel, L., and DuBois, R. N. (2006) Cyclooxygenase-1-derived PGE2 promotes cell motility via the G-protein-coupled EP4 receptor during vertebrate gastrulation. *Genes Dev.* **20,** 77–86
44. Matsuoka, Y., Li, X., and Bennett, V. (2000) Adducin: structure, function and regulation. *CMLS Cell. Mol. Life Sci.* **57,** 884–895
45. Ivaska, J., Pallari, H. M., Nevo, J., and Eriksson, J. E. (2007) Novel functions of vimentin in cell adhesion, migration, and signaling. *Exp. Cell Res.* **313,** 2050–2062
46. Dascher, C., and Balch, W. E. (1996) Mammalian Sly1 regulates syntaxin 5 function in endoplasmic reticulum to Golgi transport. *J. Biol. Chem.* **271,** 15866–15869
47. Nechiporuk, A., Poss, K. D., Johnson, S. L., and Keating, M. T. (2003) Positional cloning of a temperature-sensitive mutant emmental reveals a role for sly1 during cell proliferation in zebrafish fin regeneration. *Dev. Biol.* **258,** 291–306
48. Kim, S. W., Park, J. I., Spring, C. M., Sater, A. K., Ji, H., Otchere, A. A., Daniel, J. M., and McCrea, P. D. (2004) Non-canonical Wnt signals are modulated by the Kaiso transcriptional repressor and p120-catenin. *Nat Cell Biol.* **6,** 1212–1220
49. te Velthuis, A. J., and Bagowski, C. P. (2007) PDZ and LIM domain-encoding genes: molecular interactions and their role in development.

ScientificWorldJournal **7,** 1470–1492
50. Ott, E. B., Sakalis, P. A., Marques, I. J., and Bagowski, C. P. (2007) Characterization of the enigma family in zebrafish. *Dev. Dyn.* **236,** 3144–3154
51. Weiser, D. C., Pyati, U. J., and Kimelman, D. (2007) Gravin regulates mesodermal cell behavior changes required for axis elongation during zebrafish gastrulation. *Genes Dev.* **21,** 1559–1571
52. Millard, T. H., Dawson, J., and Machesky, L. M. (2007) Characterisation of IRTKS, a novel IRSp53/MIM family actin regulator with distinct filament bundling properties. *J. Cell Sci.* **120,** 1663–1672
53. Watabe-Uchida, M., John, K. A., Janas, J. A., Newey, S. E., and Van Aelst, L. (2006) The Rac activator DOCK7 regulates neuronal polarity through local phosphorylation of stathmin/Op18. *Neuron* **51,** 727–739
54. Pinheiro, E. M., and Gertler, F. B. (2006) Nervous Rac: DOCK7 regulation of axon formation. *Neuron* **51,** 674–676
55. Nellist, M., Burgers, P. C., van den Ouweland, A. M., Halley, D. J., and Luider, T. M. (2005) Phosphorylation and binding partner analysis of the TSC1-TSC2 complex. *Biochem. Biophys. Res. Commun.* **333,** 818–826
56. Lemeer, S., Ruijtenbeek, R., Pinkse, M. W., Jopling, C., Heck, A. J., den Hertog, J., and Slijper, M. (2007) Endogenous phosphotyrosine signaling in zebrafish embryos. *Mol. Cell. Proteomics* **6,** 2088–2099